315. The Influence of Friction on the Dynamic Model for a 6-DOF Parallel Robot with Triangular Platform

Tiberiu-Pavel Itul[1,a], Doina Liana Pisla[1,b]
[1]Technical University of Cluj-Napoca, Constantin Daicoviciu 15, RO-400020 Cluj-Napoca, Romania
[a]itultp@yahoo.com, [b]doinapisla@yahoo.com

(Received 14 September 2007; accepted 22 October 2007)

Abstract. The dynamic analysis is an important element of the mechanical design and control of parallel mechanisms. This paper presents a method for the dynamical modeling of the guided in three points parallel robots with six degrees of freedom having triangular platform, including the friction. The evaluation of the full generalized forces is performed in two stages. In the first stage, the drive generalized forces are established, based on the dynamical equations without friction. Using the Newton-Euler equations, the reactions from each joint are computed. In the second stage the additional drive generalized forces due to the frictions from the active and passive joints are computed by means of two approaches. The first approach considers the whole mechanism. The generalized additional forces which include the friction effect from the corresponding drive joints and the friction effect from all passive joints are calculated using principle of virtual power and the mechanism Jacobi matrices. The second approach treats the kinematic chains as independent. The generalized additional forces are evaluated using the virtual work principle. In both approaches the passive joints are approximated with compliant joints whose momentum are equal to the friction torques of these joints.
Keywords: parallel robots, kinematics, dynamics, friction.

Introduction

Dynamics effects and analysis are the basis of design specification and advanced control of parallel mechanical systems. To establish the equations of motion, there exist essentially four methods: Newton-Euler equations; Lagrange equations of first kinds with so-called LAGRANGE multipliers; Lagrange equations of second kind with a minimum number of system coordinates; Virtual work formulation.

In [1] different solutions for solving the dynamical model for the guided in three points parallel robots are presented.

Until now, in the most existing papers, the experimental identification of dynamics for the parallel robots is restricted to simple models in combination with adaptive control algorithms. The most important force source which is not included is the friction. Few authors have also approached the dynamic model considering the friction forces too. This gap was closed by a new approach presented in [2], where Grotjahn develops a complex dynamic model including friction, which uses Jourdain's principle of virtual power and is suited for the parallel robot control of the innovative hexapod PaLiDA. The friction model includes friction in both active joints as well in passive joints. Poignet et al. [3] deal with the application of the interval analysis to estimate the 4-degrees of freedom parallel robot dynamic parameters. Yiu et al [4] developed the dynamic modeling including friction for a planar 2-dof redundant parallel robot.

Riebe et al. [5] present a dynamic model for a Stewart platform with six DOF, based on Newton-Euler equations including the frictional behaviour. The parameters describing the friction model are identified and optimized. Chen et al. [6] present a dynamic model of a Cartesian guided tripod including the nonlinear compliance and mechanical friction. Quantitative analysis and comparison of the variation friction sources from the actuated joints and passive joints have been conducted.

It is estimated that the forces due to the friction represent about 25% from the forces/torques which are necessary for the manipulator movement in typical situations. Thus it is necessary to model these friction forces in order to reflect in the dynamic equations the physical reality.

For the friction forces approximation two models could be applied: the model of the viscous friction in which the force/torque (Q_{fv}) due to the friction is in proportion to the joint movement speed and the model of Coulomb friction in which the force/torque (Q_{fc}) due to the friction is in proportion to the normal reaction on the joint axis.

$$Q_{fv} = c\dot{q}\ ;\ Q_{fc} = \mu_r \frac{d}{2} N \operatorname{sgn}(\dot{q}) \text{ - in rotational joint;}$$

$$Q_{fc} = \mu N \operatorname{sgn}(\dot{q}) \text{ - in prismatic joint.} \quad (1)$$

© VIBROMECHANIKA. JOURNAL OF VIBROENGINEERING. 2007 OCTOBER/DECEMBER, VOLUME 9, ISSUE 4, ISSN 1392-8716

These two models together lead to a more reasonable approximation of the effects due to the friction:

$$Q_f = Q_{fv} + Q_{fc}. \quad (2)$$

The parallel mechanisms contain also passive joints. The forces/torques which must be applied in the kinematical axes should be supplemented with the friction effect from these passive joints.

In the paper is proposed a method for the additional forces evaluation from the drive joints due to the friction from the drive and passive joints. The proposed method for the supplementary forces evaluation considers the friction effect from the all driving and passive joints of the mechanism. The passive joints are approximated with compliant joints which have the momentum equal with the friction torques from these joints.

The evaluation of the generalized forces is performed in two stages. In the first stage the drive generalized forces are established which are based on the dynamical equations without friction.

Based on Newton-Euler the reactions from each joint are computed. In the second stage are computed the additional drive generalized forces due to the frictions from the active and passive joints.

Kinematic modeling of guided in three points parallel structures

The structural scheme of a guided in three points parallel mechanisms with 6 DOF is presented in the figure 1 [7]. The circles surrounding the joints, which are located in the proximity of the fixed base suggest that these joints are actuated, each of them having 1 DOF.

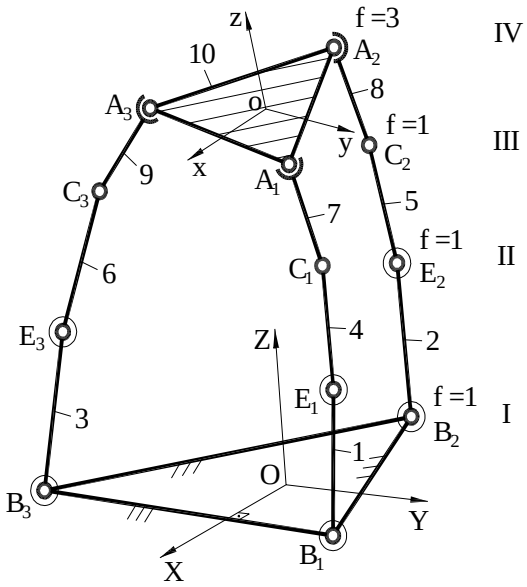

Fig. 1. The structural archetype scheme

Each kinematic chain, which connects the fixed base with the mobile platform, contains also a passive joint with 1 DOF and a passive spherical joint with 3 DOF (guiding point). Each of them is moving with respect to the fixed base on a mobile 2-DOF curve.

As application it was chosen the 3-PPRS parallel manipulator (figure 2).

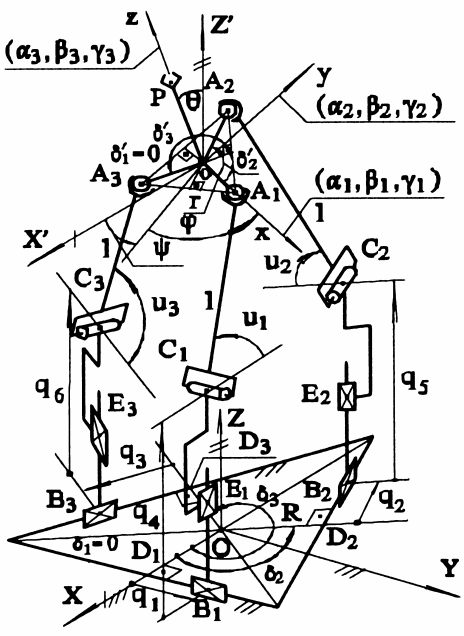

Fig. 2. The 3-PPRS parallel structure

The points B_i (i=1,2,3) and E_i (i=1,2,3) represent active prismatic joints, whereas the revolute joints and ball joints are located in C_i (i=1,2,3) respectively in A_i (i=1,2,3). The six prismatic joints are actuated, the rest of them being passive. The geometric parameters R , r and l represent: radius of fixed base, radius of the working platform (WP) and length of the guiding rods C_iA_i, and $\delta_1' = \delta_1 = 0^0; \delta_2' = \delta_2 = 120^0; \delta_3' = \delta_3 = 240^0$ represent the angles between kinematic chains from the WP and the fixed base level.

To solve the geometric problems, Itul and Pisla [2] use the method of input-output (I-O) equations. The I-O equations are the relations between the joint coordinates (q_i and q_{i+3}; i=1,2,3) and the world coordinates of the working platform (WP), X,Y, Z, α, β, γ :

$$\left(\mathbf{P}_i - \mathbf{P}_{Ci}\right)^2 - l^2 = 0; \left(\mathbf{P}_i - \mathbf{P}_{Ci}\right) \cdot \mathbf{n}_i = 0; \; i = 1,2,3. \quad (3)$$

where: $\mathbf{P}_i(X_i, Y_i, Z_i)$ is radius vector from the base frame center O to the guiding point A_i; $\mathbf{P}_{Ci}(X_{Ci}, Y_{Ci}, Z_{Ci})$ is radius vector from the point O to joint C_i center; $\mathbf{n}_i$ is the unit vector of C_i joint axis. In this case the inverse geometrical model has an analytical solution, which involves a second degree algebraic equation solving and

the geometrical direct model can be only numerically solved by using the Newton-Raphson method.

To find the kinematic model (KM), the I-O equations are derived with respect to time yielding to:

$$[A]\dot{\mathbf{q}} = [B]\dot{\mathbf{X}} \tag{4}$$

where: $\dot{\mathbf{q}}(\dot{q}_1, \dot{q}_2, \dot{q}_3, \dot{q}_4, \dot{q}_5, \dot{q}_6)$ is the driving velocity vector, $\dot{\mathbf{X}}(\dot{X}, \dot{Y}, \dot{Z}, \omega_X, \omega_Y, \omega_Z)$ is the end-effector velocity vector, $[A]$ and $[B]$ are Jacobi matrices, $\mathbf{P}(X, Y, Z)$ is the radius vector from the point O to the o mobile platform center.

While the inverse kinematic model ($\dot{\mathbf{q}} = [A]^{-1}[B]\dot{\mathbf{X}}$) has an analytical solution, the direct kinematic model ($\dot{\mathbf{X}} = [B]^{-1}[A]\dot{\mathbf{q}}$) can be only numerically solved, that means it requires the discrete definition of the matrix $[B]$ for the mobile platform pose parameters and then its numerical inversion.

Dynamics without friction

The proposed algorithm for the inverse dynamic model without friction consists from four steps, as following:

Step 1. The guiding bar C_iA_i of the kinematic chain "i" is separated from the system (figure 3).

The theorem of the angular momentum with respect to the mobile axis of the rotation joint C_i allows the deriving of the W_i component of the reacting force from the spherical joint, which is normal on the plane defined by the rotation joint axis and the guiding bar:

$$W_i = \frac{1}{2} m_b (g + \ddot{q}_{i+3}) cu_i + \frac{1}{3} m_b l \ddot{u}_i \tag{5}$$

Step 2. The mobile platform is separated from the rest of the mechanism (figure 4).

The Newton-Euler equations, which model the moving of the mobile platform, are the following:

$$\begin{aligned} &(M+m)\mathbf{a}_o = (M+m)\mathbf{g} + \sum_{i=1}^{3}(\mathbf{H}_i + \mathbf{V}_i + \mathbf{W}_i); \\ &[I]\boldsymbol{\varepsilon} + \boldsymbol{\omega} \times [I]\boldsymbol{\omega} = \sum_{i=1}^{3} \mathbf{oA}_i \times (\mathbf{H}_i + \mathbf{V}_i + \mathbf{W}_i) \end{aligned} \tag{6}$$

where:

$\mathbf{a}_0$ is the acceleration of the point o; $\mathbf{g}$ is the gravity acceleration vector; $\mathbf{H}_i$ is the vector component of the A_i spherical joint reacting force, which is parallel to the C_i joint axis; $\mathbf{V}_i$ is the vector component of the A_i spherical joint reacting force, which lies along the C_iA_i guiding rod; $\mathbf{W}_i = W_i \mathbf{w}_i$ is the vector component of the A_i spherical joint reacting force, which is normal on the plane defined by the joint rotation axis C_i and the rod C_iA_i; $[I]$ is the inertia matrix of the mobile platform. The equations (6) allow obtaining the reaction components H_i and V_i from the spherical joints with respect to the kinematic parameters of the mobile platform.

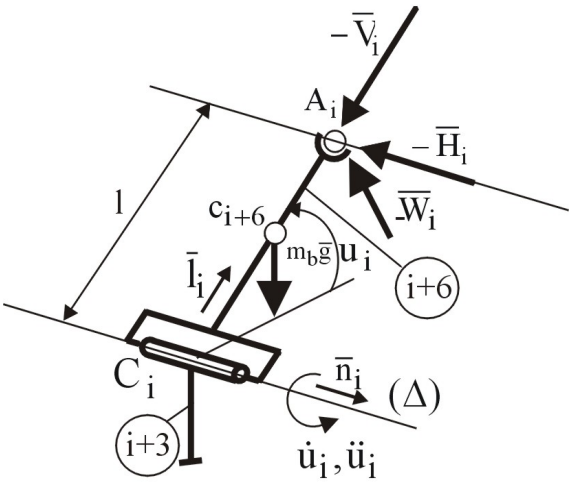

Fig. 3. Dynamic equilibrium of the A_iC_i guiding rod

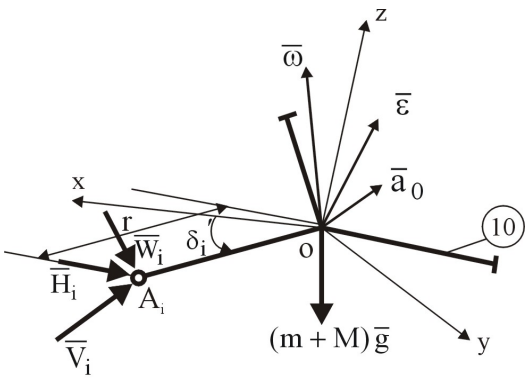

Fig. 4. Step 2

Step 3. The $E_iC_iA_i$ kinematic chain is separated and all the forces are introduced similarly to the steps 2 and 3 (figure 5). By projecting the moving equations of the mass centre on the B_i, the generalized force Q_{i+3} is derived:

$$\begin{aligned} Q_{i+3} = {} & (m_{i+3} + m_b)(\ddot{q}_{i+3} + g) + m_b \frac{l}{2}(\ddot{u}_i\, cu_i - \dot{u}_i^2\, su_i) + \\ & + V_i\, su_i - W_i\, cu_i \end{aligned} \tag{7}$$

The "i" element mass was noted with "m_i", the "i+3" with "m_{i+3}" and the guiding rod mass with "m_b".

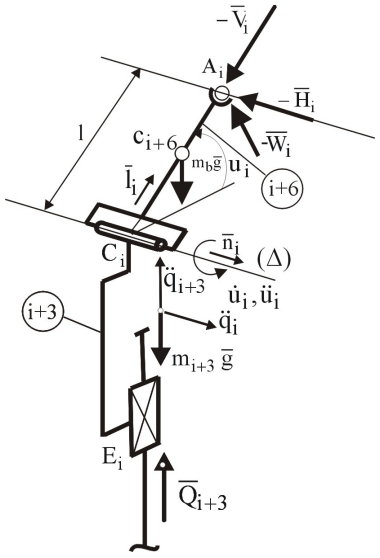

Fig. 5. Step 3

Step 4. The $B_iE_iC_iA_i$ kinematic chain is also separated (figure 6). The moving equation of the mass center with respect to the joint axis E_i yields the generalized actuating force Q_i:

$$Q_i = (m_i + m_{i+3} + m_b)\ddot{q}_i + H_i \qquad (8)$$

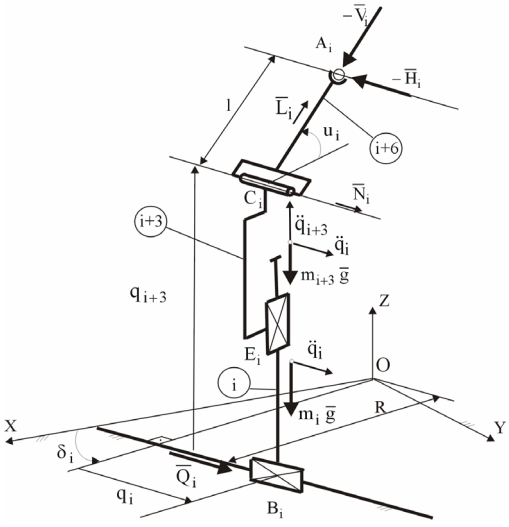

Fig. 6. The $B_iE_iC_iA_i$ kinematic chain

Dynamics with computation of the additional drive generalized forces due to the frictions

A friction torque in a passive joint is a vector, which is situated along the relative rotational speed of the considered link with respect to the neighboring links and it has opposite direction to this relative speed (fig. 3) [8]:

$$\mathbf{M}_{si} = -\left(c_s\boldsymbol{\omega}_{ri} + \mu_s\frac{d_s}{2}\frac{\sqrt{H_i^2+V_i^2+W_i^2}}{|\boldsymbol{\omega}_{ri}|}\boldsymbol{\omega}_{ri}\right) = -k_{si}\boldsymbol{\omega}_{ri};$$

$$\mathbf{M}_{ri} = -\left(c_r\dot{\mathbf{u}}_i + \mu_r\frac{d_r}{2}\frac{\sqrt{(V_i^*)^2+(W_i^*)^2}}{|\dot{\mathbf{u}}_i|}\dot{\mathbf{u}}_i\right) = -k_{ri}\dot{\mathbf{u}}_i;$$

$$H_i^* = H_i + m_b\ddot{q}_i;$$

$$V_i^* = V_i su_i - W_i cu_i + \frac{1}{2}m_b l(\ddot{u}_i cu_i - \dot{u}_i^2 su_i) + m_b(g + \ddot{q}_{i+3})$$

$$W_i^* = V_i cu_i + W_i su_i - \frac{1}{2}m_b l(\ddot{u}_i su_i + \dot{u}_i^2 cu_i) \qquad (9)$$

The following notations were made: H_i, V_i, W_i - the reaction force components from the spherical joint considering the model without friction; $\mathbf{M}_{si}$ - the friction moment from the spherical joint A_i; c_s - the viscous friction coefficient from the spherical joint; μ_s - the Coulomb friction coefficient from the spherical joint; d_s - the diameter of the spherical joint ball; $\boldsymbol{\omega}_{ri} = \dot{\mathbf{u}}_i - \boldsymbol{\omega}$ - the relative angular speed of the guiding bar A_iC_i with respect to the mobile plate; $\dot{\mathbf{u}}_i = \dot{u}_i\mathbf{n}_i$ - the absolute angular speed of the guiding bar A_iC_i; $\boldsymbol{\omega}$ - the absolute angular speed of the mobile plate; $\mathbf{M}_{ri}$ - the friction moment from the passive rotation joint C_i; c_r - the viscous friction coefficient from the rotational joint C_i; μ_r - the Coulomb friction coefficient from the joint C_i; d_r - the diameter of the rotational joint spindle; m_b - the guiding bar mass, g - gravity acceleration, c - cosine; s - sine.

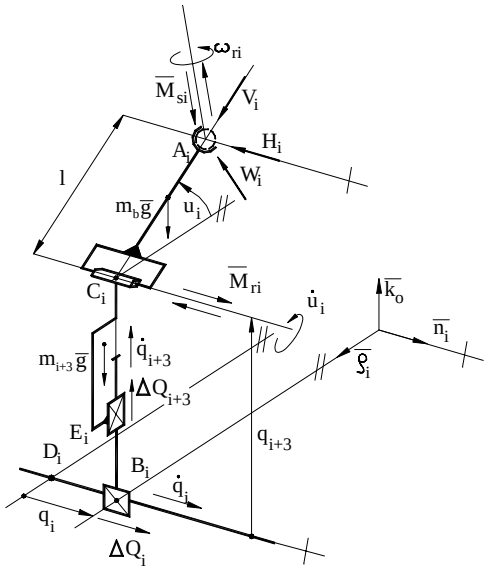

Fig. 7. The "i" kinematic chain

The first approach assumes the propagation of the virtual displacements, applied to the drive joints to all passive joints of the mechanism, respectively that a displacement of an active joint involves displacements in all passive joints of the mechanism.

Through the differentiation of the closure equations for the direct geometrical model is obtained the relation between the drive joint speeds and the passive joint speeds:

$$[A_u]\dot{\mathbf{q}} = [B_u]\dot{\mathbf{u}};\ \dot{\mathbf{u}} = [J_u]\dot{\mathbf{q}};\ [J_u] = [B_u]^{-1}[A_u];$$

$$\dot{\mathbf{q}} = [\dot{q}_1, \dot{q}_2, ..., \dot{q}_6]^T,\ \dot{\mathbf{u}} = [\dot{u}_1, \dot{u}_2, \dot{u}_3]^T. \tag{10}$$

The direct kinematical model has the form:

$$\dot{\mathbf{X}} = [J]\dot{\mathbf{q}};\ [J] = \begin{bmatrix} J_X \\ J\omega \end{bmatrix} = [B]^{-1} \cdot [A];$$

$$\dot{\mathbf{X}} = [\dot{X}, \dot{Y}, \dot{Z}, \omega_X, \omega_Y, \omega_Z]^T. \tag{11}$$

In order to get the generalized drive forces which are necessary to overcome the frictions from the passive joints is applied the principle of the virtual power. Finally it yields:

$$\begin{aligned} &[\Delta Q_1^p, \Delta Q_2^p, \Delta Q_3^p, \Delta Q_4^p, \Delta Q_5^p, \Delta Q_6^p]^T = \\ &= [J_u]^T \cdot \begin{bmatrix} (k_{r1} + k_{s1})\dot{u}_1 - 2k_{s1}\overline{\omega} \cdot \overline{n}_1 \\ (k_{r2} + k_{s2})\dot{u}_2 - 2k_{s2}\overline{\omega} \cdot \overline{n}_2 \\ (k_{r3} + k_{s3})\dot{u}_3 - 2k_{s3}\overline{\omega} \cdot \overline{n}_3 \end{bmatrix} + \\ &+ (k_{s1} + k_{s2} + k_{s3})[J_\omega]^T \cdot \begin{bmatrix} \omega_X \\ \omega_Y \\ \omega_Z \end{bmatrix} \end{aligned} \tag{12}$$

where: c_t is the viscous friction vector from the active prismatic joint; μ is the sliding friction coefficient from the same joint.

The second approach assumes that the virtual displacements applied to the drive joints are propagating only to the mobile platform level. The generalized drive forces which are necessary to overcome the frictions from the passive joints are obtained by using the virtual work principle:

$$\Delta Q_i^p = -\frac{M \cdot k_0}{lcu_i};\ \Delta Q_{i+3}^p = -\frac{(M_{si} + M_{ri}) \cdot n_i}{lcu_i}. \tag{13}$$

In both approaches the necessary drive generalized forces for the specified displacement performance have the form:

$$\begin{aligned} &Q_i^m = Q_i + \Delta Q_i^m + \Delta Q_i^p; \\ &Q_{i+3}^m = Q_{i+3} + \Delta Q_{i+3}^m + \Delta Q_{i+3}^p,\ i = 1,2,3. \end{aligned} \tag{14}$$

where $Q_i, Q_{i+3}\ (i = 1,2,3)$ are the generalized drive forces, which have been obtained with the inverse dynamical model without friction and ΔQ_i^m and ΔQ_{i+3}^m are the additional forces due to the frictions from the active joints:

$$\begin{aligned} &\Delta Q_i^m = c_t \dot{q}_i + \\ &+ \mu\sqrt{(W_i^*)^2 + \left[V_i^* + (m_i + m_{i+3})g + m_{i+3}\ddot{q}_{i+3}\right]^2} \cdot \\ &\cdot \operatorname{sgn}(\dot{q}_i), \end{aligned} \tag{15}$$

$$\begin{aligned} &\Delta Q_{i+3}^m = c_t \dot{q}_{i+3} + \\ &+ \mu\sqrt{\left(H_i^* + m_{i+3}\ddot{q}_i\right)^2 + \left(W_i^*\right)^2}\ \operatorname{sgn}(\dot{q}_{i+3}). \end{aligned} \tag{16}$$

Some simulation results

The new dynamic algorithms including friction effects based on the above presented approaches have been implemented in a simulation program for the 3-PPRS parallel robots with the fixed base at the bottom. For more accurate approximation of the dry friction, in the developed program was taken into account the modulus of the relative velocity.

The chosen input data for the parallel robot are: R =0,15 m, l =0,30 m, r =0,10 m, $\delta_1 = \delta_1' = 0^o$, $\delta_2 = \delta_2' = 120^o$, $\delta_3 = \delta_3' = 240^o$, M =1 kg, the manipulated object mass m =1 kg, the actuators masses: $m_1 = m_2 = m_3 = m_4 = m_5 = m_6 =$ 0,5 kg, the guiding bars masses m_b=0,2 kg.

The selected displacement of the working platform is a helical translation:

$$X(t) = R \cdot \cos(\lambda(t));\ Y(t) = R \cdot \sin(\lambda(t));$$

$$Z(t) = .5 + .1\frac{\lambda(t)}{2 \cdot \pi}$$

where

$$\lambda(t) = \begin{cases} \frac{2}{\pi} \cdot t^2 & \text{if } 0 \le t < \frac{\pi}{2} \\ 2 \cdot \left(t - \frac{\pi}{2}\right) + \frac{\pi}{2} & \text{if } \frac{\pi}{2} \le t < \pi \\ -2 \cdot \frac{(t-\pi)^2}{\pi} + 2 \cdot (t - \pi) + 3 \cdot \frac{\pi}{2} & \text{if } \pi < t \le \frac{3\pi}{2} \end{cases}$$

$$\psi = \theta = \varphi = 0$$

In the figure 8 are represented the generalized drive forces Q_{1n} and Q_{1n}^m for the motor 1 considering the simplified model without friction respectively the new model considering the friction forces.

The following input data have been considered:

$$c_t = 0.0015\ N \cdot s/m;\ c_r = 0.02\ N \cdot m \cdot s/rad;$$
$$c_s = 0.02\ N \cdot m \cdot s/rad;\ \mu = 0.05;\ d_r = 0.01 m;$$
$$d_s = 0.016 m;\ \mu_p = 0.1;\ s = 0.00005 m;$$

$$\mu_r = \mu_p + \frac{2s}{d_r} / \sqrt{1+\mu_p^2};\ \mu_s = \frac{1}{3}\mu_p .$$

In the figure 9 are represented the motor 1 additional forces due to the friction (global force $\Delta Q1_n$, forces due to the friction from the active and passive joints $\Delta Q1m_n$ respectively $\Delta Q1p_n$). For the imposed mobile platform displacement, both approaches have lead to the same values of additional forces due to the frictions from the passive joints in the base robot driving joints.

Generally, if the mobile platform displacement is a translational one, the results obtained through these two approaches are alike or identical.

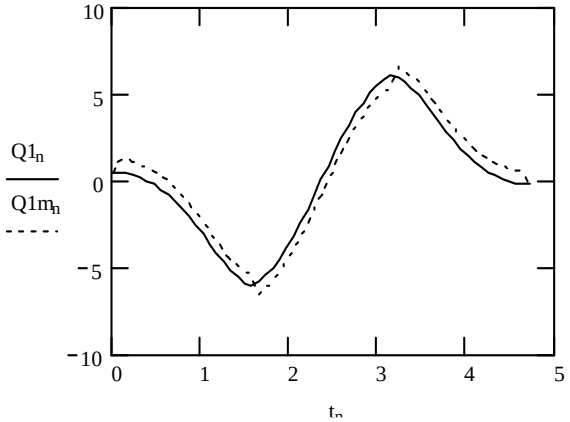

Fig. 8. The generalized drive forces

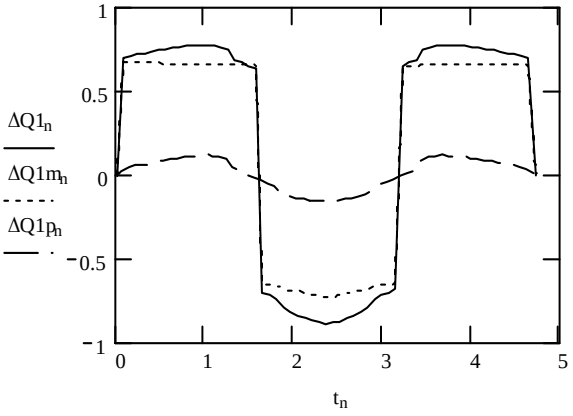

Fig. 9. The additional forces

Conclusions

The dynamic modeling of 6 DOF parallel robots considering the friction effects is a difficult problem. The integration of the friction results in the mathematical model will lead to better results close to the real behavior of the robot. The used method in this paper considers either the whole mechanism or imaginary independence of the kinematics chains.

The obtained numerical results have shown that the frictions from the drive joints have substantial effect in the additional drive forces components. Although the second approach is more simple and faster (the Jacobi matrices computation is not involved), in the additional force evaluation are introduced significant errors in such configurations, in which the u_i angles are nearby from the right angles (the connection kinematic chains are straight or almost straight). Generally, the numerical results have shown that the friction coefficient from the passive joints do not significantly influence the additional drive forces.

The proposed algorithms are relatively simple, clear and compact. The work presented in this paper is important because the developed dynamical algorithms including friction, based on kinematical algorithms offer the possibility of a more complex dynamic study of these parallel robots in order to evaluate their dynamic capabilities and to generate efficient control algorithms.

References

[1] Itul T., Pisla D. and Pisla A. On the Solution of Inverse Dynamics for 6-DOF Robot with Triangular Platform, in 1st European Conference on Mechanism Science, EUCOMES, ISBN 3-901249-85-0 (on CD), Obergurgl, Austria, February 21–26, (2006).

[2] Grotjahn M., Heimann B. and Abdellatif H. Identification of Friction and Rigid-Body Dynamics of Parallel Kinematic Structures for Model-Based Control, in Multibody System Dynamics, (11)3: 273-294, (2004).

[3] Poignet Ph., Ramdani N. and Vivas O. A. Robust estimation of parallel robot dynamic parameters with interval analysis, in 42nd IEEE Conference on Decision and Control, pages 6503-6508, Hawaii USA, 2003.

[4] Yiu Y. K., and Li Z. X. Dynamics of a Plannar 2-dof Redundant Parallel Robot, In International Conference on Mechatronics Technology, 2001, Singapore, 339-343.

[5] Riebe S., Ulbrich H. Modelling and online computation of the dynamics of a parallel kinematic with six degrees-of-freedom, Archive of Applied Mechanics, 72: 817-829, 2003.

[6] Chen J.-S., Kuo, Yao-Hung, Hsu W.-Y. The influence of friction on contouring accuracy of a Cartesian guide tripod machine tool, Int. J. Adv. Manuf. Technol, 30:470-478, (2006).

[7] Plitea N. Kinematische Synthese von verzweigten räumlichen Getrieben mit Sechspunktführung der Industrieroboter mit sechs Freiheitsgraden vom Typ I. In 5th IFToMM International Symposium on Linkages and CAD Methods, II-1:483-494, Bucharest, (1989).

[8] Itul T., Pisla D. and Pisla A. Dynamic Model of a 6-DOF Parallel Robot by Considering Friction Effects, in 12th IFToMM World Congress, Besançon (France), June 18-21, CD-ROM edition, (2007).